Journal for ImmunoTherapy of Cancer

Novel peptide-based oncolytic vaccine for enhancement of adaptive antitumor immune response via co-engagement of innate Fcγ and Fcα receptors

Sara Feola ,[1,2,3,4] Firas Hamdan ,[1,2,3,4] Salvatore Russo ,[1,2,3,4] Jacopo Chiaro,[1,2,3,4] Manlio Fusciello ,[1,2,3,4] Michaela Feodoroff,[1,2,3,4] Gabriella Antignani,[1,2,3,4] Federica D'Alessio,[1,2,3,4] Riikka Mölsä ,[1,2,3,4] Virpi Stigzelius,[1,2,3,4] Paolo Bottega,[1,2,3,4] Sari Pesonen,[5] Jeanette Leusen ,[6] Mikaela Grönholm,[1,2,3,4] Vincenzo Cerullo [1,2,3,4,7]

To cite: Feola S, Hamdan F, Russo S, *et al*. Novel peptide-based oncolytic vaccine for enhancement of adaptive antitumor immune response via co-engagement of innate Fcγ and Fcα receptors. *Journal for ImmunoTherapy of Cancer* 2024;**12**:e008342. doi:10.1136/jitc-2023-008342

► Additional supplemental material is published online only. To view, please visit the journal online (https://doi.org/10.1136/jitc-2023-008342).

SF and FH are joint first authors.

Accepted 18 February 2024

For numbered affiliations see end of article.

Correspondence to
Professor Vincenzo Cerullo; vincenzo.cerullo@helsinki.fi

ABSTRACT

Background Cancer immunotherapy relies on using the immune system to recognize and eradicate cancer cells. Adaptive immunity, which consists of mainly antigen-specific cytotoxic T cells, plays a pivotal role in controlling cancer progression. However, innate immunity is a necessary component of the cancer immune response to support an immunomodulatory state, enabling T-cell immunosurveillance.

Methods Here, we elucidated and exploited innate immune cells to sustain the generation of antigen-specific T cells on the use of our cancer vaccine platform. We explored a previously developed oncolytic adenovirus (AdCab) encoding for a PD-L1 (Programmed-Death Ligand 1) checkpoint inhibitor, which consists of a PD-1 (Programmed Cell Death Protein 1) ectodomain fused to an IgG/A cross-hybrid Fc. We coated AdCab with major histocompatibility complex (MHC-I)-restricted tumor peptides, generating a vaccine platform (named PeptiCab); the latter takes advantage of viral immunogenicity, peptide cancer specificity to prime T-cell responses, and antibody-mediated effector functions.

Results As proof of concept, PeptiCab was used in murine models of melanoma and colon cancer, resulting in tumor growth control and generation of systemic T-cell-mediated antitumor responses. In specific, PeptiCab was able to generate antitumor T effector memory cells able to secrete various inflammatory cytokines. Moreover, PeptiCab was able to polarize neutrophils to attain an antigen-presenting phenotype by upregulating MHC-II, CD80 and CD86 resulting in an enhanced T-cell expansion.

Conclusion Our data suggest that exploiting innate immunity activates T-cell antitumor responses, enhancing the efficiency of a vaccine platform based on oncolytic adenovirus coated with MHC-I-restricted tumor peptides.

WHAT IS ALREADY KNOWN ON THIS TOPIC

⇒ For cancer vaccine, the innate immune system is crucial to orchestrate an appropriate adaptive immune response to control tumor growth.

WHAT THIS STUDY ADDS

⇒ The coactivation of innate Fcγ and Fcα receptors, via the expression of an IgGA (half-IgG and half-IgA) Fc fusion peptide, enhances the T-cell immune response induced by an adenovirus-based cancer vaccine.

HOW THIS STUDY MIGHT AFFECT RESEARCH, PRACTICE OR POLICY

⇒ This study demonstrates the use of the IgGA-Fc fusion peptides can be used in parallel with adenovirus-based cancer vaccine to improve T-cell immune responses to better control tumor growth should be tested in the clinics.

INTRODUCTION

The crucial role of the immune system in protecting against nascent neoplasms has just been fully exploited in recent decades, giving rise to the cancer immunotherapy field. Cancer immunotherapy ranges from chimeric antigen receptor-T cells to tumor-infiltrating lymphocytes, which have significantly improved the overall survival of many patients with cancer. Moreover, among active cancer immunotherapeutic approaches, cancer vaccination has been extensively used to generate antitumor responses.[1] Cancer therapeutic vaccines aim to create or stimulate (or both) T-cell-mediated antitumor responses. To bolster the adaptive immune response, a cancer vaccine requires an adjuvant to stimulate antigen-presenting cells (APCs) and a target to guide response specificity. Different platforms have been explored for this application such as viruses like particles, nanoparticles, subunit vaccines, and viral vectors. Depending on the nature and utilization, the use of a specific platform is

preferred. For instance, subunit vaccines are used for infectious diseases, generating primarily innate immune response to prevent viral infections. In contrast, adenoviral vectors elicit cellular immune responses, harnessing a robust cytotoxic T lymphocyte response.[2] This feature is preferred for designing cancer therapeutic vaccines. Indeed, viruses used as platforms to modulate the immune response exploit the intrinsic immunogenicity of pathogen physiology and host-pathogen interactions. APCs express pattern recognition receptors (PRRs), such as toll-like receptors, that bind pathogen-associated molecular patterns (PAMPs). On this interaction, maturation, enhanced phagocytosis, and release of proinflammatory cytokines are induced. Adenoviral DNA works as a PAMP that is recognized by PRRs, which results in activation of the innate immune system (mainly dendritic cells (DCs) and natural killer (NK)) and initiation of inflammatory processes, making adenoviral vectors an ideal platform for tumor antigen delivery.

We have previously developed a platform named PeptiCRAd, which consists of an oncolytic adenovirus decorated with major histocompatibility complex (MHC)-I-restricted peptides.[3] Positively charged MHC-I restricted tumor peptides (poly-lysine tail-peptides) are attached to the adenoviral capsid through electrostatic interactions.[3] Our technology combines the viral immunogenicity and the cancer specificity, which is dictated by the tumor peptides used for coating the adenoviral capsid. Our technology has shown efficacy in a murine model of melanoma,[4] triple-negative breast cancer[5] and colon cancer,[6] using either unarmed adenovirus or adenovirus encoding immunostimulatory molecules such as CD40L and OX40L.[7] Here we explored our adenovirus-based vaccine using an adenovirus encoding a PD-L1 (Programmed-Death Ligand 1) checkpoint inhibitor.

A robust adaptive immune response against tumors also relies heavily on an effective innate immune response. Passive antibody therapy is crucial in activating the innate immune system and facilitates a stronger adaptive immune response against cancer.[8 9] This effect has been demonstrated in both murine models and human patients treated with anti-HER2 therapy.[10] Furthermore, patients treated with anti-MUC1 monoclonal antibody have been able to generate a strong cellular immune response against MUC1.[11] One mechanism behind this enhancement is the engagement of activating Fcγ receptors found on APCs (such as DCs), which induces maturation, cross-presentation, upregulation of co-stimulatory molecules, and antigen presentation.[12] Subsequently, the activation of Fc triggers pro-inflammatory signaling, leading to an upregulation of MHC/co-stimulatory molecules and soluble factors that influence T-cell activation and maturation.[8]

We have engineered an oncolytic adenovirus, AdCab, which expresses a novel PD-L1 checkpoint inhibitor.[13 14] AdCab consists of a PD-1 ((Programmed Cell Death Protein 1) ectodomain fused to an IgGA cross-hybrid Fc, which incorporates regions of IgG1 and IgA. Currently, all therapeutic anticancer antibodies in clinical use are of the IgG isotype, which is excellent at activating the complement system, NK cells, and engaging APCs. However, they fail to activate the most abundant leukocyte population, neutrophils, due to the expression pattern of Fc-gamma (Fcγ) receptors. Although neutrophils express the activating receptor FcγRIIa, they have a much higher expression of the non-signaling FcγIIIb (CD16b) and some expression of inhibitory FcγIIb (CD32b).[15 16] In contrast, IgA can exploit this neutrophil population due to the expression of the activating Fcα (CD89) receptor. Neutrophils are professional phagocytes that possess various advantages over other APCs, such as early migration and high numbers at inflammation sites. This population has been shown to cross-prime both CD4+ and CD8+ T cells[17–19] and is an attractive target for vaccines. Therefore, the IgG/A cross-hybrid Fc can generate effector functions of both IgG1 and IgA, leading to enhanced tumor killing and possibly activation of multiple APCs. Consequently, we coated AdCab with MHC-I-restricted tumor peptides, creating a vaccine platform named PeptiCab. We demonstrated that this complex retained oncolytic activity, antibody production, and antibody-mediated effector functions. Adoptive cell transfer (ACT) from human CD89 transgenic mice into recipient mice showed that the neutrophil population elicited an antitumor response on AdCab treatment. PeptiCab was then tested for its antitumor activity in an animal model of melanoma and demonstrated control of tumor growth. When PeptiCab was used in a model of colon cancer, both primary and secondary malignant lesions were contained, indicating the generation of a systemic antitumor response. Immunological analysis in mice revealed that PeptiCab generated an antigen-specific response in T cells within the effector memory compartment. Additionally, the neutrophil population exhibited a reduced exhaustion profile (PD-L1 expression) and enhanced expression of co-stimulatory molecule CD86 and MHC-II complex, suggesting a role for neutrophils as APCs.

Overall, our data demonstrated that an adenovirus-based cancer vaccine designed to elicit antigen-specific response benefits from antibody-mediated effector functions. In particular, we observed enhanced antigen-specific T-cell generation within the effector compartment. Second, neutrophil analysis revealed that the observed population may play a role as possible APCs, improving treatment with cancer therapeutic vaccines.

RESULTS

AdCab decorated with tumor peptides preserves both stability and oncolytic fitness

We compared AdCab to PeptiCab to investigate whether coating AdCab with polyK-tail peptides influenced virus aggregation. To accomplish this, we analyzed the complex by nano-tracking analysis. As expected, AdCab showed a significant amount of aggregation, with a peak around

100 nm (online supplemental figure 1A). PeptiCab had a similar aggregation profile, almost identical to AdCab (online supplemental figure 1B). These data suggested that the polyK-tail peptide and AdCab could be mixed with no additional aggregating effect. Next, oncolytic activity was analyzed on coating AdCab with polyK-tail peptides. Human lung carcinoma cells (A549) and human triple-negative breast cancer cells (MDA-MB-436) were infected with Ad5/3Δ24 (unarmed), AdCab or PeptiCab. Oncolysis was observed in both cell lines (A549 and MDA-MB-426) in a dose-dependent manner (online supplemental figure 1C, D). As human adenoviruses infect murine cell lines but are unable to replicate, we infected murine melanoma (B16K1 and B16F10), triple-negative breast cancer (4T1), and colon cancer (CT26) cell lines to further corroborate PeptiCab oncolytic activity. No cell death was observed, confirming that oncolytic fitness was unaffected by the addition of polyK-tail peptides in AdCab (online supplemental figure 1E–H). We then investigated the antibody production in AdCab compared with PeptiCab. The supernatants from A549 and B16K1 infected with Ad5/3Δ24 (unarmed virus), AdCab or PeptiCab were collected 1 day apart after infection (day 1, day 2 and day 3) and analyzed for the presence of fusion antibody. Fusion antibody was produced in a time-dependent manner (online supplemental file 1I, J). Overall, the data confirmed that the coating of AdCAb with polyK-tail peptides allowed normal oncolytic activity; moreover, the antibody production was unaffected, supporting the use of PeptiCab as an oncolytic adenovirus encoding Fc-fusion antibody.

Tumor peptide decoration on AdCab does not affect Fc-effector mechanisms

After observing that decorating AdCab with peptides did not affect oncolytic fitness or Fc-fusion peptide production, we decided to test whether the Fc-fusion peptide maintains Fc-dependent effector mechanisms such as antibody-dependent cellular cytotoxicity (ADCC) and complement-dependent cytotoxicity. We plated five different target cells (online supplemental figure 2A, B, human cell lines, online supplemental figure 2C–E, murine cell lines) and infected them with AdCab, PeptiCab, and unarmed Ad5/3 virus for 2 days. Following incubation, we co-incubated various effector cells (online supplemental figure 2 “PBMCs or PMNs”) or combinations of effector cells (online supplemental figure 2 “PBMCs+PMNs”) since the Fc can induce effector mechanisms of both IgA and IgG (online supplemental figure 2). Additionally, we added serum to activate the complement system in the presence of both PBMCs (Peripheral blood mononuclear cells) and PMNs (Polymorphonuclear neutrophils) to observe the enhanced antitumor activity of the Fc-fusion peptide (online supplemental figure 2 “All”). Both AdCab and PeptiCab exhibited a similar trend, with comparable levels of specific lysis when PBMCs or PMNs were added. Moreover, a higher level of specific antibody-mediated lysis was observed when both effector populations were present and was further increased when serum was added to AdCab or PeptiCab-treated cells. As expected, no specific cell lysis was demonstrated with the unarmed virus, indicating that cell death was due to Fc-effector mechanisms and not viral oncolysis. This demonstrates that PeptiCab retains Fc-effector mechanisms despite the peptide decoration.

PeptiCab shows therapeutic activity in an in vivo model of murine melanoma and modulates T-cell-specific immune responses

We wanted to assess in a preliminary experiment the antibody-mediate antitumor activity by blood effector cells in vivo. To achieve this, we used transgenic mice (TG-mice) expressing a human FcαRI (CD89) in their PMN population (eg, neutrophils). An established murine melanoma model (B16.OVA) was intratumorally pretreated either with Adeno unarmed or AdCab (figure 1A). Mice were then intratumorally injected with bone marrow (BM) and splenocytes harvested from TG-mice; BM and splenocytes from wild type mice were used as controls. Mice-bearing tumors pretreated with AdCAb and injected with BM and splenocytes derived from TG-mice (AdCab+huCD89) showed remarkable tumor growth control (figure 1B) when compared with the other groups, as shown also in the analysis of the area under the curve (AUC) (figure 1C). These results suggested the IgA-mediated killing ability of neutrophils in vivo. Moreover, when we dissected the neutrophils population (figure 1D–F), we observed the upregulation of the co-stimulatory marker CD86 and MHC-II molecules in tumors of mice preconditioned with AdCab and adoptively injected with human CD89-expressing neutrophils compared with the control groups. Next, we implemented PeptiCRAd, using AdCab decorated with tumor peptides, generating PeptiCab. PeptiCab was tested in a murine model of melanoma in a proof-of-concept experiment. Incompetent C57B/l mice were subcutaneously injected with melanoma tumor cells from the B16.K1 syngeneic model in the right flank. Once the tumors were established, AdCab mixed with the clinically relevant melanoma antigen polyK-TRP2 (PeptiCab) was used to intratumorally treat the mice. Phosphate-buffered saline (PBS) alone (Mock group) or PeptiCRAd (Adeno unarmed mixed with polyK-TRP2) were used as controls. Analysis of tumor growth revealed that both PeptiCRAd and PeptiCab were effective (figure 1G). Next, we examined the immunological background of these mice. T-cell functional characterization by enzyme-linked immunospot (ELISpot) assay revealed that PeptiCab increased the generation of TRP2 specific immune responses compared with PeptiCRAd and even more compared with Mock (figure 1H). Spleen analysis by flow cytometry indicated that both the CD4 (figure 1I) and CD8 (figure 1J) T-cell compartments were unaffected by the treatments. However, the generation of CD8+TRP2 was increased (figure 1K) in the PeptiCab group, confirming the ELISpot data. When we analyzed the tumor microenvironment (TME), we observed that

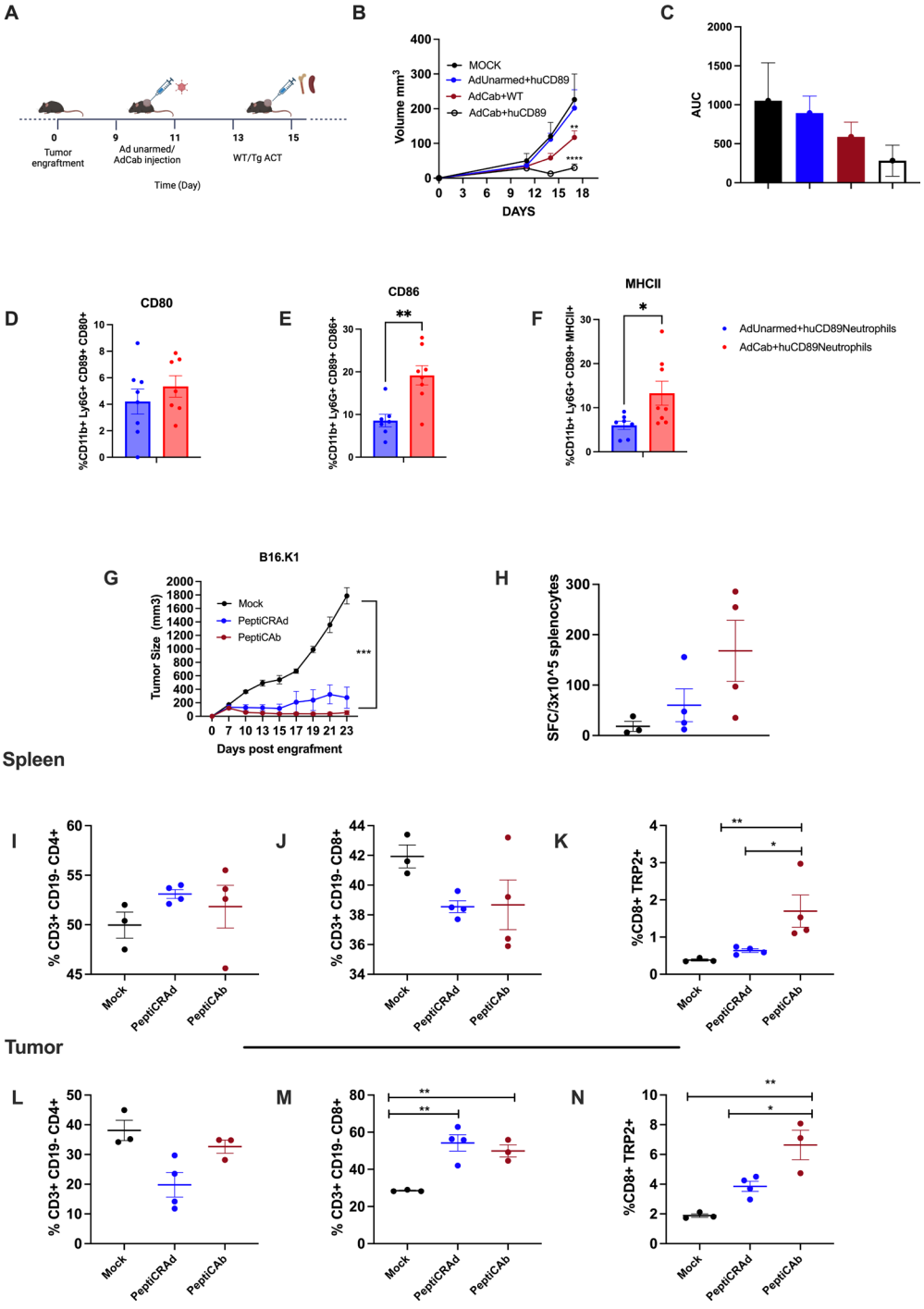

Figure 1 PeptiCab technology combines IgGA cross-hybrid Fc activity and antigen-specific T-cell response generation. A schematic representation of the experiment is shown. Mice were subcutaneously injected with B16.OVA at day 0 and pretreated with AdUnarmed or AdCab at days 9 and 11. Adoptive cell transfer (ACT) of WT or TG immune components was performed at days 13 and 15 (A). Tumor growth is represented as mean±SEM for each treatment group (B). The area under the curves relative to the tumor growth in mice was calculated and plotted as the mean±SD (C). Flow cytometry analysis of CD80 (D) CD86 (E) and MHC-II (F) was performed; data are shown as percentages for each population. PBS (Mock), PeptiCRAd and PeptiCab treatments were given intratumorally at days 9, 11, 13 and 21 post tumor implantations. Tumor size is presented as the mean±SEM (G). Enzyme-linked immunospot analysis revealed the generation of TRP2 antigen-specific analysis. Mice were indicated as scatter dot plots on background correction. (H) Flow cytometry analysis of spleens and tumors was performed at the end of the experiments (day 23) the frequency of CD4+ (I) CD8 (J) and TRP2+CD8 (K) is reported in the spleen and the frequency of CD4+ (L) CD8+ (M) and TRP2+CD8+ (N). All the data are plotted as dot plots for each mouse and each treatment group. Statistical significance was assessed with two-way ANOVA (*p≤0.05; **p≤0.01; ***p≤0.001; ****p≤0.0001; ns, non-significant) for the tumor growth and with one-way ANOVA for the flow cytometry analysis (*p≤0.05; **p≤0.01; ***p≤0.001; ****p≤0.0001; ns, non-significant). ACT, adoptive cell transfer; ANOVA, analysis of variance; AUC, area under the curve; MHC, major histocompatibility complex; TG, transgenic mice; WT, wild-type.

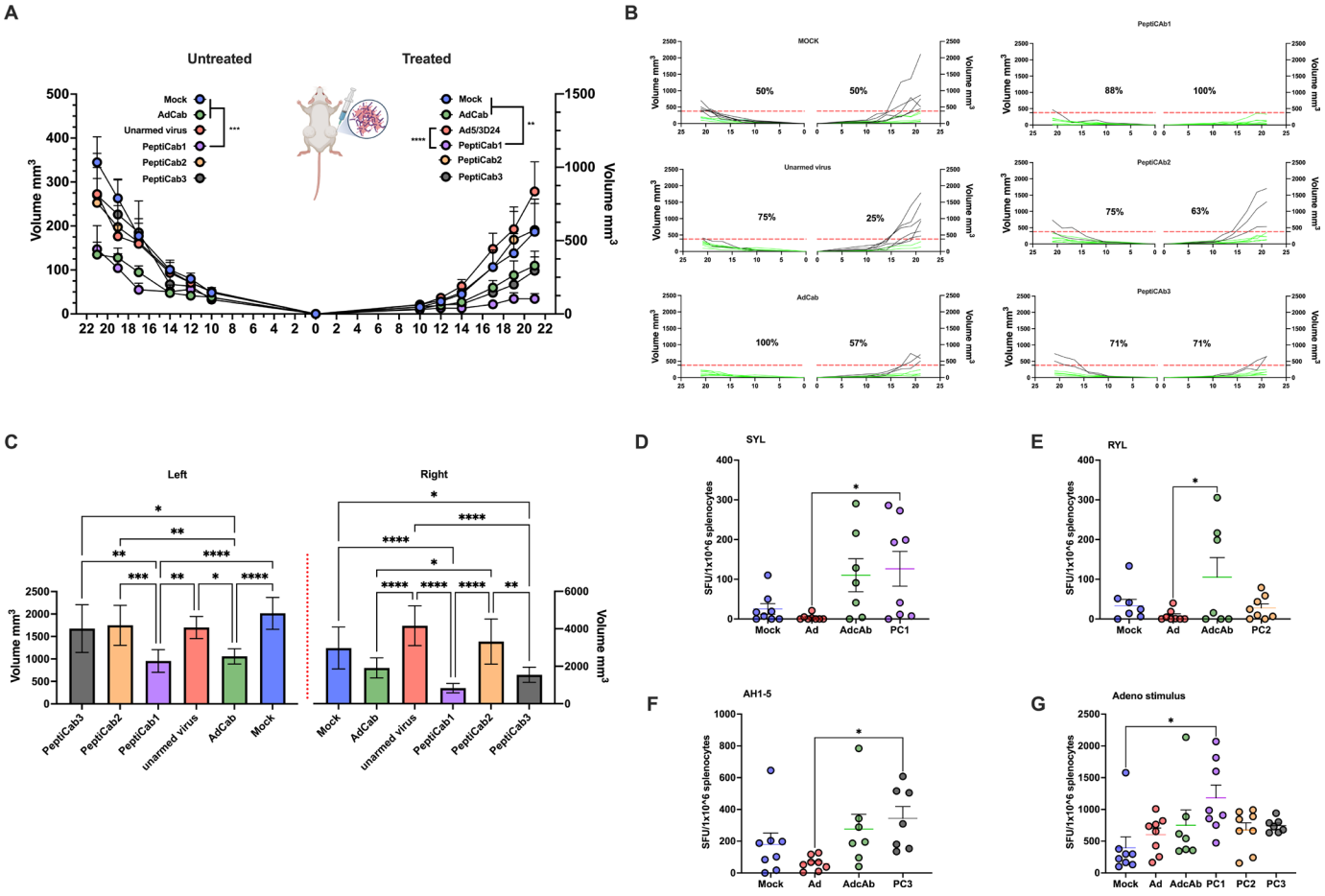

Figure 2 PeptiCab technology generates systemic antitumor immune response. BALB/c mice (n=8) were subcutaneously injected with 1×10^6 and 0.6×10^6 cells in the right and in the left flank, respectively. At day 10 post implantation, the right tumor was treated four (or three) times with PeptiCab (AdCab mixed with polyK peptides). The left tumor was left untreated. Mock and AdCab alone were used as controls. Tumor growth is shown as mean±SEM. Statistical difference was assessed with two-way ANOVA (*p≤0.05; **p≤0.01; ***p≤0.001; ****p≤0.0001; ns, non-significant) (A). Single tumor growth for each mouse, for each treatment group, and for left and right tumor is shown in the panel. The overall median of the Mock group was used as a threshold (red dotted line) to define the percentage of responders (green) and non-responders (black) (B). The area under the curve was calculated for the tumor growth for each treatment group and is shown as bar plots (mean±SD) (C). Splenocytes harvested from mice were functionally investigated by enzyme-linked immunospot interferon-γ analysis in the presence of SYLPPGTSL (D) RYLPAPTAL (E) SPSYAYHQF (F) or adenovirus (G) at the end of the experiment (day 21). The panel shows the stimuli conditions and the treatment groups. The frequencies of antitumor T-cell responses are depicted as peptides-specific reaction per 1×10^6 splenocytes on background correction. Statistical analysis was performed with one-way ANOVA for flow cytometry analysis (*p≤0.05; **p≤0.01; ***p≤0.001; ****p≤0.0001; ns, non-significant). ANOVA, analysis of variance.

the CD4 compartment was unaffected by the different treatment regimens (figure 1L). Conversely, an increased infiltration of CD8 T cells within the TME was observed (figure 1M); TRP2 pentamer analysis showed significative generation of CD8+TRP2 specific-T cell in the PeptiCab-treated group (figure 1N). Taken together, these data indicate that PeptiCab technology combined the antibody-mediated activity and modulation of the T-cell compartment, generating antigen-specific T cells.

PeptiCab stimulates a systemic antitumor immune response, controls untreated secondary lesions, and modulates T-cell memory compartment

The preliminary data prompted us to explore further whether PeptiCab generates a systemic antitumor response by modulating the immune compartment. To this end, syngeneic BALB/c mice were injected in both flanks with the colon tumor model CT26. Once the tumors appeared, the left tumors were left untreated and the right tumors were treated with AdCAb coated with single peptides, previously discovered in our previous immunopeptidomic investigations[6] (PeptiCab1 (PC1), AdCab mixed with polyK-SYLPPGTSL and PeptiCab2 (PC2), AdCab mixed with polyK-RYLPAPTAL). Mice treated with PBS (Mock), Adeno unarmed (Ad5/3Δ24), or AdCab were used as controls. Additionally, we treated a group of mice with AdCab mixed with PolyK-SPSYAYHQF PeptiCab3 (PC3). This peptide is derived from $gp70_{423–431}$ (AH1-5), a known immunodominant antigen of CT26 derived from a viral envelope glycoprotein encoded in the genome, and it was used as an additional internal

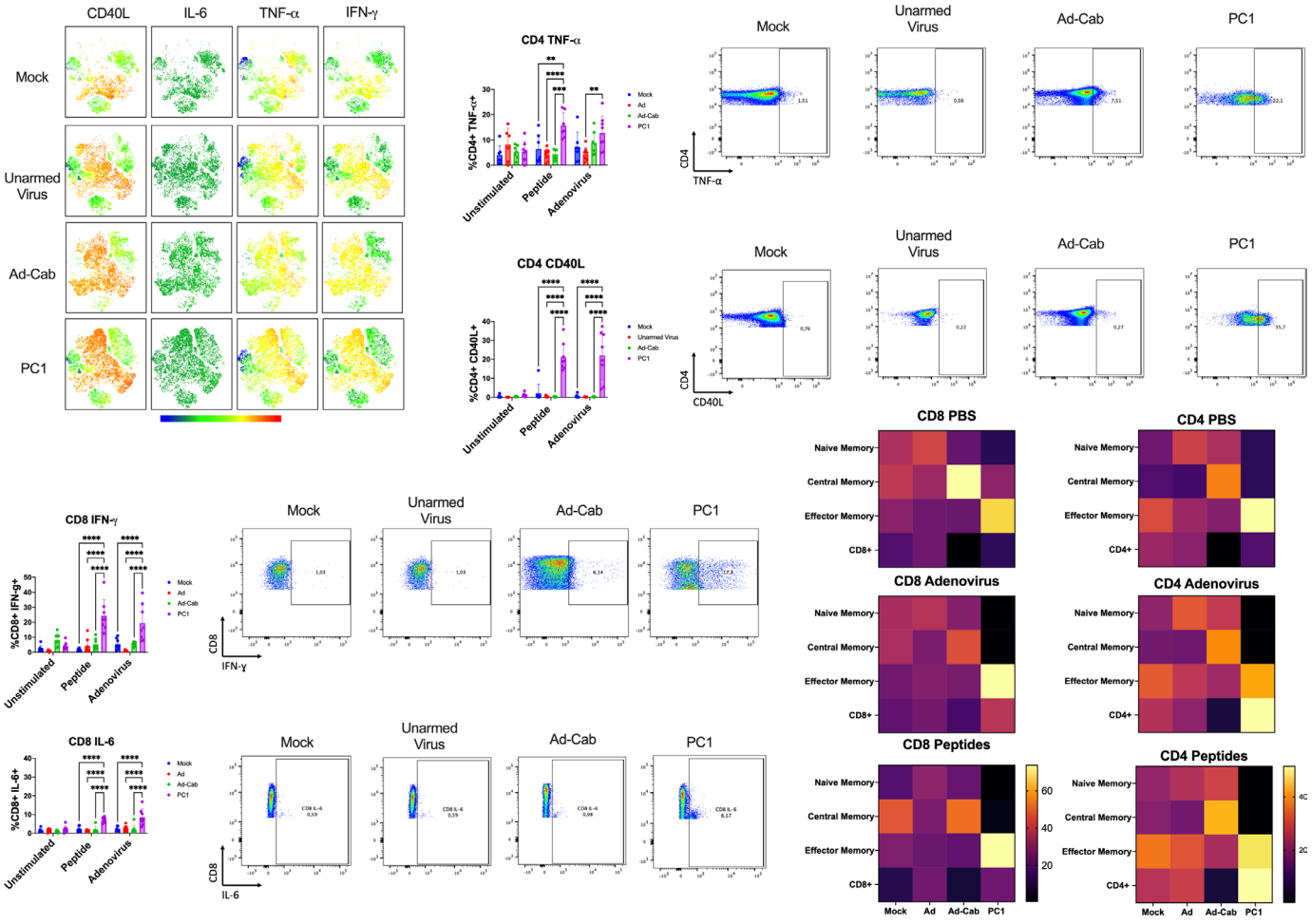

Figure 3 PeptiCab technology induces immune response against tumor antigens. t-distributed stochastic neighbor embedding plots of CD3+T cells show the density of IL-6, CD40L, TNF-α and IFN-γ (A) release of different treatment groups stimulated with SYL peptide was performed. Individual measurements of CD4+T cell release of TNF-α and CD40L (B) under different stimulant (media, SYL peptide, or 20 MOI of Ad5/3) are shown. Flow cytometry dot plots measuring the release of TNF-α and CD40L release (C) from CD4+T cells from different treatment groups exposed to SYL peptide are shown. The amount of IFN-γ and IL-6 (D) release from CD8+T cells was measured in different treatment groups when exposed to media, SYL peptide, or 20 MOI of Ad5/3. Flow cytometry dot plots of the release of IFN-γ and IL-6 (E) from CD8+T cells when different treatment groups were exposed to SYL peptide are shown. Heat maps showing the percentages of different T-cell memory cells in CD8+T cells (F, H, J) and CD4+ (G, I, K) compartment on exposure to media, SYL peptide, or 20 MOI of Ad5/3. All the analyses were performed at the end of the experiment (day 21). IFN, interferon; IL, interleukin; PBS, phosphate-buffered saline; MOI; multiplicity of infection; TNF; tumor necrosis factor.

control for the experimental conditions. Among the treatment groups, PeptiCab1 showed tumor growth control in the treated tumors (figure 2A); interestingly, antitumor response was reported also in the untreated lesion in both AdCab and PeptiCab1 (figure 2A). The data were confirmed by analyzing single tumor growth from a single mouse for each treatment group (figure 2B) and by AUC analysis (figure 2C). Next, we investigated the generation of antigen-specific T-cell responses. Splenocytes were harvested from mice treated with different regimens and functionally investigated by ELISpot. On peptide-specific stimulation, upregulation of interferon (IFN)-γ-producing cells was observed in the PC1 (figure 2D) and in PC3 (figure 2F) groups. In contrast, no significative differences were observed in IFN-γ-producing cells in the PC2 group (figure 2E). Moreover, PeptiCab1 released the greatest amount of IFN-γ-producing cells on adenoviral stimulus (figure 2G) among the treatment groups.

Based on these data, we decided to explore the systemic immune response elicited by different treatments such as Mock, unarmed virus, AdCab and PC1. First, we isolated splenocytes from each group and we stimulated them with media, Ad5/3 virus, or SYLPPGTSL peptide. When we analyzed the CD3+ population after stimulation with SYLPPGTSL peptide, we observed upregulation in TNF-α (Tumor Necrosis Factor), IFN-γ and CD40L in the PC1 treatment group when compared with the other groups (figure 3A). On further investigation, CD4+T cells secreted higher levels of TNF-α and CD40L in the PC1 (figure 3B,C) treatment group when stimulated both with Ad5/3 virus and SYLPPGTSL peptide. No upregulation of IFN-γ or interleukin (IL)-6 was observed. A similar

trend was seen with the CD8+T cells, where an increase in IFN-γ and IL-6 was observed in the PC1 treatment group stimulated with Ad5/3 virus and SYLPPGTSL peptide (figure 3D) as also shown in the flow cytometry dot plots (figure 3E). However, no increase in either IFN-γ in CD4+T cells or TNF-α in CD8+T cells was observed among groups with either stimulant (online supplemental figure 3A, B).

We then investigated the memory phenotype in the spleen on stimulation. We observed a difference in T-cell memory populations among treatment groups is noticed in the absence of stimulant (media). A higher central CD8+memory T-cell compartment (CD44+C-D62L+CCR7+) was observed with the AdCab group, while a higher frequency of CD8+effector memory T cells (CD44+CD62L- CCR7−) was observed in the PC1 treatment group (figure 3F). This pattern was also observed within the CD4+memory T-cell compartment (figure 3G). Interestingly, when the stimulants were changed from media to Ad5/3 virus or SYLPPGTSL peptide, the central memory CD8+ and CD4+ T cells downregulated CD62L and became effector memory T cells in the PC1-treated group. This was not the case with the other treatment groups when stimulated either with Ad5/3 virus or SYLPPGTSL peptide (figure 3H–K). After observing an overall increase in pro-inflammatory cytokines in the PC1 group, we sought to determine the cell types responsible for the release of such cytokines (online supplemental figure 4). For CD40L, we observed that the effector memory CD4+T cells were responsible for this release in the PC1 group when stimulated with either Ad5/3 or SYLPPGTSL peptide (online supplemental figure 5, effector memory CD4). Within the effector memory CD8+T cells, upregulation of IFN-γ was observed in the PC1 group on Ad5/3 or SYLPPGTSL peptide stimulation (online supplemental figure 5, effector memory CD8). These data indicate that most of the pro-inflammatory cytokines were released when stimulated with either Ad5/3 or SYLPPGTSL peptide originate from the effector memory T cells.

To further demonstrate that CD8+T cells were responsible for the abscopal effects observed, we repeated the same experiment with PeptiCab1, termed PeptiCab in this experiment, while removing CD8+T cells before treatment. Mice were first implanted with CT26 in both flanks and then given isotype control or anti-CD8 antibodies and followed-up every other day (online supplemental figure 6A). Right tumors were then only treated with PeptiCab or PBS and the left tumors were untreated and measured. To confirm that CD8+T cells were depleted, at day 10 CD8 and CD4 T-cell population were analyzed in the peripheral blood of mice. As expected, mice given anti-CD8 antibody had a complete removal of CD8+T cells from the peripheral blood day (online supplemental figure 6B). It showed that mice with CD8+T cells and treated with PeptiCab had the best tumor control in the right flank while when removing CD8+T cells this effect was removed day (online supplemental figure 6C). This phenomenon was also seen with the left tumors, demonstrating that the abscopal effects from PeptiCab were mediated by CD8+T cells.

Mouse model expressing human FcαR recapitulates PeptiCab translational therapeutic efficacy

PeptiCab generated antigen-specific T cells and induced systemic antitumor responses. To further explore the potential translational therapeutic activity of PeptiCab, we investigated the antibody-mediated effector functions of AdCab in our cancer vaccine platform. However, mice do not express FcαRI (CD89), which is essential for IgA-mediated effector functions (Antibody dependent cell mediated cytotoxicity, Antibody dependent cell mediated phagocytosis, antigen presentation, neutrophil extracellular traps) in myeloid cells, particularly in neutrophils. Therefore, we used human Fc alpha receptor transgenic BALB/c mice. First, we subcutaneously injected CT26 on the right flank; once the tumors were established, we intratumorally injected PeptiCab (AdCab mixed with polyK-SYLPPGTSL). Mock (PBS) and PeptiCRAd (unarmed adenovirus mixed with polyK-SYLPPGTSL) were used as controls. Of note, the dose of Ad5/3Δ24 was 10-fold lower than in the previous animal experimental setting. PeptiCab treatment-controlled tumor growth in comparison to Mock and PeptiCab, suggesting that the additional presence of IgA-mediated effector functions played a key role in triggering antitumor responses at lower dosages (figure 4A). The results were also confirmed by analyzing the single tumor growth for each mouse and for each treatment group (figure 4B) and by AUC analysis (figure 4C). Indeed, in the PeptiCab group, 89% of the mice showed tumor growth control, in contrast to Mock (50%) and PeptiCRAd (67%) (figure 4D–F) during the follow-up period.

These data prompted us to further investigate the immunological status in mice on treatments with different regimens. Splenocytes were harvested and stimulated with media, Ad5/3 virus (adenovirus), or SYLPPGTSL peptide (SYL_peptide). On simulation with adenovirus or peptide, CD8+T cells in the PeptiCab group released the greatest amount of IFN-γ among the treatment groups; as well, CD40L production in the CD4+T cells compartment was also higher in the PeptiCab group, as shown in t-distributed stochastic neighbor embedding (t-SNE) plot analysis (figure 5A) and summarized in bar plots (figure 5B and figure 5C). When we further investigated the CD8+T cell population releasing INF-γ, we observed that the predominant population had phenotypic markers of effector memory T cells (figure 5D) (online supplemental figure 7). These data were corroborated by the analysis of the CD4+T cell population; here, the most CD40L was released by CD4+T effector memory cells (figure 5E) (online supplemental figure 7). Interestingly,

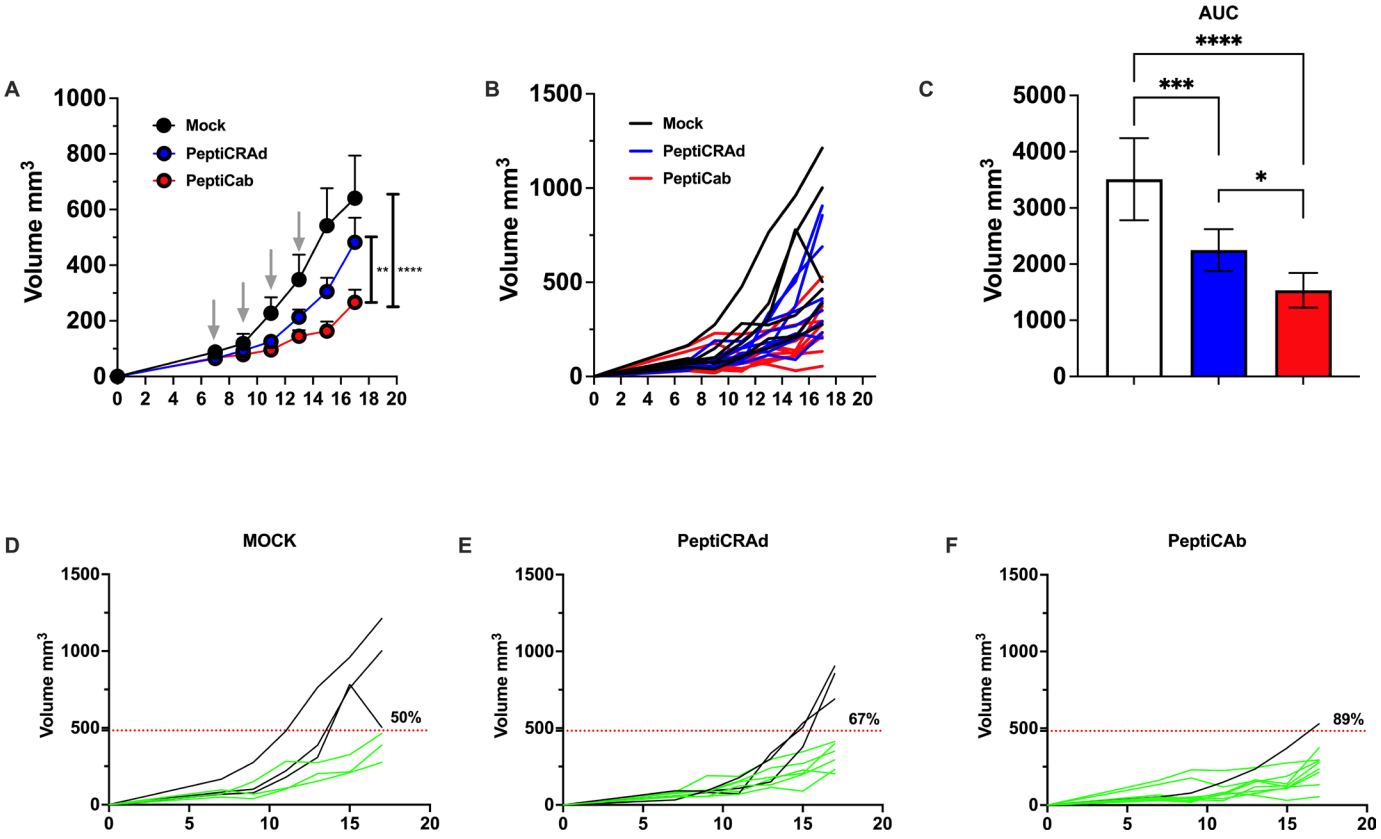

Figure 4 Human FcαR transgenic mice reveal IgA-mediated effector functions. Human FcαR transgenic BALB/c mice were subcutaneously injected on the right flank with 1×10^6 murine colon CT26 cell line. Once the tumors were established (Mock n=6, PeptiCRAd n=9, PeptiCab n=9), four intratumoral injections with PeptiCab 2 days apart (day 7,9,11, and 13 post tumor implantation) were performed. Tumor growth is shown as mean±SEM. Statistical significance was assessed by two-way analysis of variance (*p≤0.05; **p≤0.01; ***p≤0.001; ****p≤0.0001; ns, non-significant) (A). Single tumor growth from a single mouse is summarized as mean±SEM (B). The AUC was calculated for the tumor growth for each treatment group and is shown as bar plots mean±SD (C). Deconvolution for each treatment group for single tumor growth for each mouse is shown as mean±SEM. The number of responders (green) and non-responders (black) was defined based on the median tumor growth from Mock groups (red dotted line). The percentage of responders is shown for each treatment group. Tumor growth is shown as the mean±SEM (D–F). AUC, area under the curve.

on adenovirus or SYL peptide stimulation, we observed a rapid transition from CD8+T central memory cell to CD8+T effector memory cell (T_{em}) in both PeptiCRAd and PeptiCab groups (figure 5F–I).

PeptiCab enhances neutrophil activity by inducing an APC-like phenotype

We investigated the impact of hCD89 expression in mice on neutrophil activity within the TME across different treatment groups. t-SNE plots were generated, focusing on CD11b+Ly6G neutrophils and activation/inhibitory markers were examined (figure 6A). Notably, a distinct neutrophil population (highlighted with a circle) in the PeptiCab-treated group appeared to be absent when compared with the other treatment groups (figure 6A). This population exhibited high expression of PD-L1, suggesting that PeptiCab treatment led to the down-regulation of this suppressive neutrophil population. This finding was further confirmed when analyzing the percentage of PD-L1+neutrophils among treatment groups, which revealed a clear reduction in both PeptiCRAd and PeptiCab groups compared with the Mock group (figure 6B).

To assess whether the decrease in suppressive neutrophils was accompanied by upregulation of activation markers, we analyzed MHC-II, CD86, and CD80 expression on CD11b+Ly6G+ neutrophils from all treatment groups. Surprisingly, no significant differences in the expression of these activation markers were observed among the treatment groups (online supplemental figure 8A). To further explore these findings, we conducted a clustering analysis based on activation and inhibitory marker expression to identify potentially overlooked neutrophil subsets. Clustering analysis revealed an upregulation of antigen-presentation machineries, specifically MHC-II and CD86, in populations 3, 5, and 8 within the PeptiCab group when compared with the other groups (figure 6C). This suggests the existence of an upregulated antigen-presenting subset of neutrophils in the PeptiCab group.

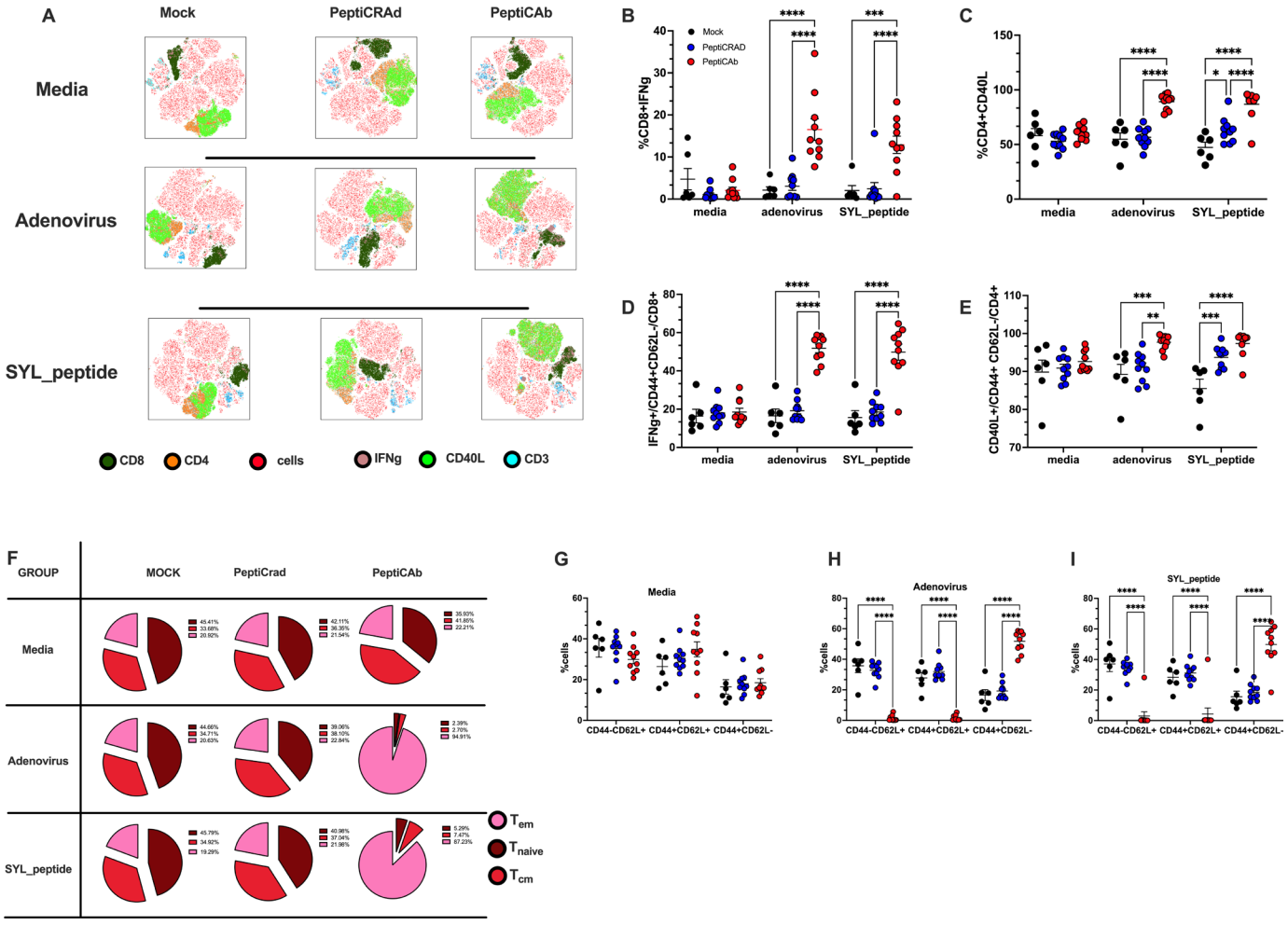

Figure 5 Transgenic mice expressing human FcαR demonstrate possible PeptiCAb translational therapeutic effect. Intracellular analysis of spleens was performed at the end of the experiments (day 17). The spleens were seeded and stimulated with media, adenovirus, or SYLPPGTSL. t-distributed stochastic neighbor embedding plot shows clusters based on flow cytometry analysis. Data sets were merged as described in the methods. Each color corresponds to one population (A). The frequency of CD8+ (B) and CD4+ (C) T cells releasing IFN-γ and CD40L is shown. The frequency of effector memory CD8+and CD4+ T cells releasing INF-γ (D) and CD40L (E) are shown. The transition from CD8+T naïve cells to CD8+T effector cells phenotype is shown as part of the whole. The percentage for each subpopulation (T_{naive}, T_{em}, and T_{cm}) is presented on the side of each graph (F). The CD8+T cells subtypes analysis is summarized in bar plots for stimulation with media (unstimulated) (G) adenovirus (H) and SYLPPGTSL (I). All data are shown as dot plots for each mouse and each treatment group and statistical significance was assessed with one-way analysis of variance with Tukey test for multiple comparisons for flow cytometry analysis (*p≤0.05; **p≤0.01; ***p≤0.001; ****p≤0.0001; ns, non-significant). IFN, interferon; T_{cm}, T central memory cell; T_{em}, T effector memory cell.

To further investigate this phenomenon, we differentiated neutrophils into mature and immature populations using CD101 (online supplemental figure 9). Generally, a higher prevalence of mature neutrophils was observed in the TME compared with immature neutrophils (online supplemental figure 8B). However, no statistically significant differences in the frequency of mature (CD11b+Ly6G+CD101+SiglecF−) or immature neutrophils (CD11b+Ly6G+CD101−SiglecF+) were found among the treatment groups (online supplemental figures 7 and 8). Of interest, when examining the immature neutrophils, we observed upregulation of both MHC-II (figure 6D) and CD86 (figure 6E) in the PeptiCab treatment group. Conversely, in the PD-L1+ mature neutrophils, no clear increase in either MHC-II or CD86 expression was observed among the treatment groups (online supplemental figure 10A). Nonetheless, when analyzing the PD-L1− mature neutrophils, we observed notable differences in MHC-II (figure 6F) and CD86 (figure 6G) expression. Specifically, the PeptiCab treatment group displayed a statistically significant upregulation of both MHC-II and CD86 compared with the other treatment groups (figure 6F,G). These data demonstrate that PeptiCab-treated mice exhibited an upregulation of MHC-II and CD86 on PD-L1− mature neutrophils, which may explain the mechanism behind the enhanced antitumor T-cell response.

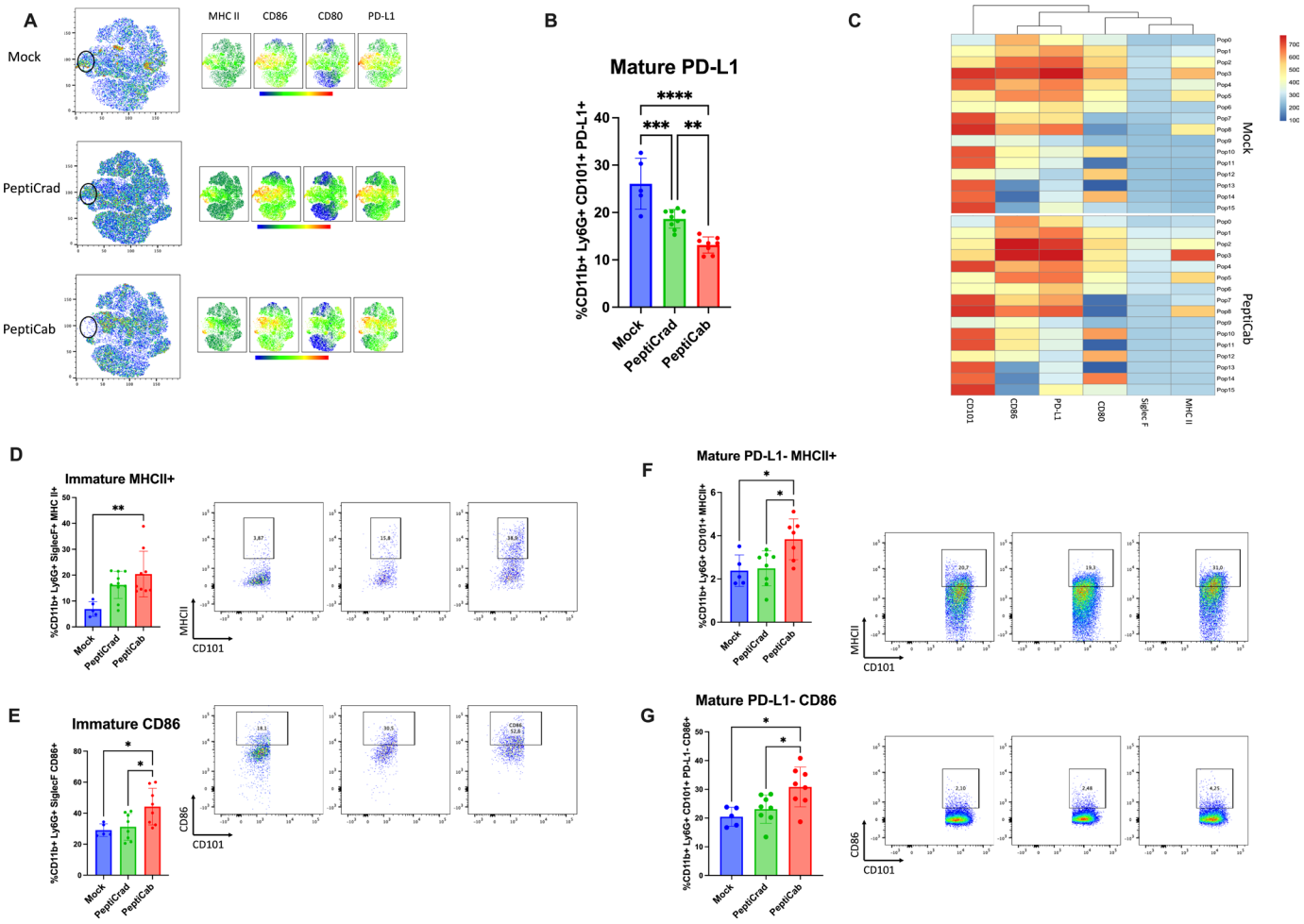

Figure 6 Neutrophils exhibit a lower anti-suppressive phenotype while attaining antigen presenting cell-like function in PeptiCab-treated mice. t-SNE plots of neutrophils along with density t-SNE plots measuring for MHC-II, CD86, CD80, PD-L1 are shown (A). Flow cytometry dot plots and individual data of PD-L1+mature neutrophils are shown (B). FlowSom analysis performed on neutrophils (CD11b+Ly6G+) using MFI measurements of CD101, CD86, PD-L1, CD80, Siglec-F, and MHC-II (C). Flow cytometry dot plots and individual data of expression of MHC-II (D) and CD86 (E) in immature neutrophils (CD11b+Ly6G+CD101+). Individual data and flow cytometry dot plots of expression of MHC-II (F) and CD86 (G) expression in mature neutrophils (CD11b+Ly6G+CD101−). Statistical significance was assessed with one-way analysis of variance with Tukey test for multiple comparisons (*p≤0.05; **p≤0.01; ***p≤0.001; ****p≤0.0001; ns, non-significant). The analysis was performed at the end of the experiment on day 17 post tumor implantation. MFI, mean fluorescent intensity; MHC, major histocompatibility complex; PD-L1, programmed cells death ligand ;t-SNE, t-distributed stochastic neighbor embedding.

Activated neutrophils, via Fc-fusion peptide, enhance CD8+T cell expansion

Having observed that PeptiCab-treated mice attained neutrophils with an APC-like phenotype (MHC-II, CD80 and CD86 upregulation) we wanted to investigate if this could contribute to the CD8 T-cell expansion observed (figure 7A). To do this, we obtained a buffy coat from a healthy individual and isolated PBMCs and neutrophils from it. Neutrophils were either kept untreated or were used in an ADCC assay using purified IgGA-Fc fusion peptide and CT26 cells, termed neutrophils-ADCC. Untreated neutrophils and ADCC-neutrophils were then taken and co-incubated with CFSE (Carboxyfluorescein succinimidyl ester) labeled isolated CD8+T cells from the PBMCs. A cocktail of adenovirus peptides and IL-2 were then added and incubated. After 4 days, CFSE staining was then measured in the CD8+T cell population to analyze the expansion. When CD8+T cells were co-incubated with neutrophils or neutrophils-ADCC with no peptide, very little expansion can be observed (figure 7B,C). Yet, when adenovirus peptides were added an increase in expansion can be observed. Interestingly, neutrophils-ADCC were shown to have a significantly higher expansion (figure 7B,C). This data demonstrates that neutrophils can induce CD8+T cell expansion and undergoing activation using the IgGA Fc-fusion peptide can enhance such phenomenon.

DISCUSSION

The induction of antitumor T-cell responses through passive antibody administration has been hypothesized for decades, primarily driven by the potential of ADCC to kill tumor cells and release tumor antigens,

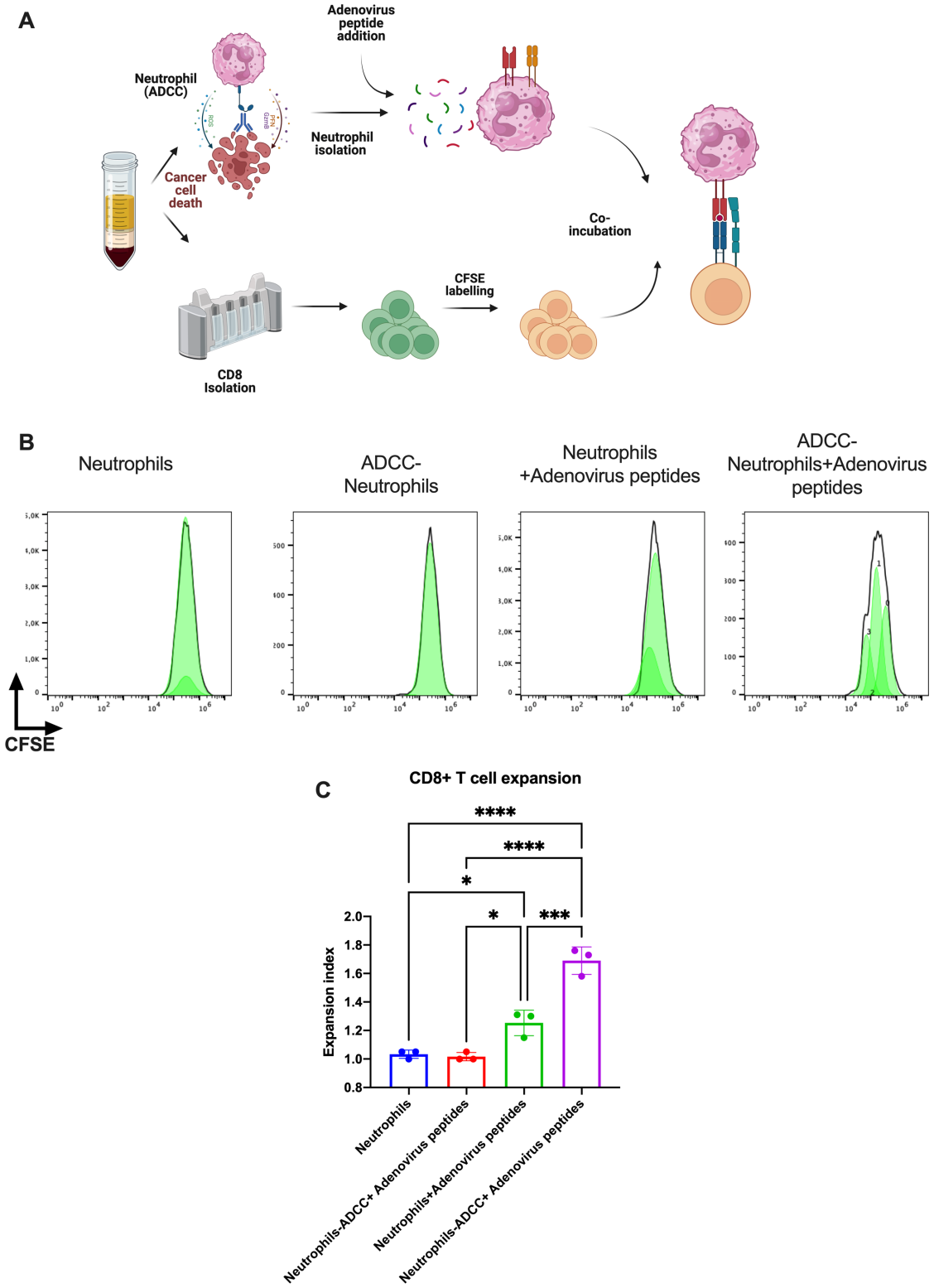

Figure 7 Neutrophils exhibit a higher CD8+T cell expansion when activated by ADCC. (A) Schematic figure demonstrating the workflow of the assay. Buffy coat from a healthy individual was separated to isolate PBMCs and neutrophils. From the PBMC layer, CD8+T cells were isolated using magnetic beads and labeled with CFSE. Neutrophils were either untreated or added in an ADCC assay with CT26 and 10 µg/mL of purified IgGA Fc-fusion peptides. Neutrophils that had underwent ADCC were termed ADCC-neutrophils. After 4 hours of ADCC, neutrophils and ADCC-neutrophils were co-incubated with CD8+T cells labeled with CFSE. 2 µg of peptides and 50 U/mL of interleukin-2 were then added and cells were incubated for 4 days. (B) Histogram plots of CD8+T cell CFSE staining. (C) Cell expansion index for each group. Statistical significance was assessed with one-way analysis of variance with Tukey test for multiple comparisons (*p≤0.05; **p≤0.01; ***p≤0.001; ****p≤0.0001; ns, non-significant). The analysis was performed at the end of the experiment on day 17 post tumor implantation. ADCC, antibody dependent-cellular cytotoxicity; PBMCs, peripheral blood mononuclear cells.

which subsequently form immune complexes with antibodies. Interestingly, these immune complexes are more efficiently processed by APCs when compared with free-roaming tumor antigens, a phenomenon facilitated by the engagement of Fcγ receptors (FcγRs) on APCs.[20 21] Dhodapkar and colleagues demonstrated that DCs internalizing tumor peptide: antibody complexes facilitated a significant expansion of antigen-specific T cells, surpassing the response induced by DCs that internalized tumor peptides alone.[22] This phenomenon not only enhanced T-cell expansion but also led to superior T-cell-mediated killing of tumor cells. The critical role of FcγRs in this context was evident, as blocking them abolished this enhanced response. Clinical studies provided further evidence, where IgG antibodies targeting CD20[23] and MUC1[11] exhibited similar immune-enhancing effects, corroborating the significance of passive antibody administration in promoting antitumor T-cell responses.

Recent studies elucidated the molecular mechanism driving these observations. DiLillo and Ravetch observed that macrophages induce tumor cell-killing through the interaction of IgG antibodies and FcγIIIA, subsequently releasing tumor peptides for opsonization.[23] This immune-complex uptake by DCs via FcγIIA interaction leads to enhanced MHC presentation, which triggers potent antitumor T-cell responses, particularly in CD20-expressing tumors. These findings offer potential explanations for observations in mice treated with AdCab, which show a higher central memory T-cell compartment (CD8 and CD4) than in PBS-treated mice. The augmented tumor killing in AdCab-treated mice may have exposed tumor antigens for efficient processing, inducing a central T-cell memory response.

CD8+T cells play a pivotal role in the anticancer immunity via cytotoxic functions. Unlike acute infections, cancer is a chronic disease, underscoring the significance of memory CD8+T cells in mediating protection against the tumor.[24] Both human and mouse studies have highlighted a positive correlation between the presence of memory T cells and the vaccine effectiveness and improved outcomes for patients. Pittet *et al* analyzed circulating CD8+T cells in patients on immunization with MEL-A; the authors demonstrated that antigen-specific CD8+T cells proliferated and had cytolytic activity accordingly with their attribute of functional memory T cells.[25] Indeed, memory CD8+T cells rapidly secrete various cytokines and possess the ability to promptly eliminate target T cells in a TCR(T-cell receptor)-dependent manner, which is a desirable effect in cancer vaccine.[24] In our in vivo study, we observed and reported a similar effect mediated by PeptiCab. The greater amount of T_{em} cells and the enhanced tumor control within the PeptiCab group indicated the generation of memory antigen-specific CD8+T. Indeed, CD8+T cells harvested from the spleen of PeptiCab-treated mice stimulated in vitro with the peptide or virus exhibited a greater IFN-γ release. Consistent with earlier findings, most of the T cells exhibited markers indicative of a memory phenotype (CD44+CD62L−). Intriguingly, a similar phenotype was observed in CD4+T cells, where production of CD40L was enhanced. These data suggest improved antigen priming mediated by PeptiCab via the greater release of CD40L from CD4+T cells and IFN-γ from CD8+T cells on peptide stimulation, indicating the generation of antigen-specific T cells. Taken together, these data indicate that PeptiCab can facilitate antigenic differentiation of CD8+T cells into memory phenotype, a desirable feature for a therapeutic cancer vaccine.

Overall, our data are consistent with clinical outcomes reported in patients with cancer. In the clinical setting, the presence of memory CD8+T cells is associated with a better prognosis. For example, the use of anti-CTLA-4 (Cytotoxic T-lymphocyte associated protein 4), ipilimumab, in the presence of higher-level memory CD8+T cells significantly increases the response rate in patients with melanoma.[26 27]

The absence of a human homologue of FcαRI in mice hinders the clinical translational potential of AdCab. Being aware of this limitation, we decided to conduct at least one tumor animal experiment by employing TG expressing human FcαRI (CD89). This extensively characterized model is a robust tool for testing the efficacy of IgA immunotherapy against infectious diseases and cancer.[28] Our aim was to elucidate the role of neutrophils in the antitumor response beyond IgG and peptide-mediated antigen T-cell generation. Consequently, we decreased the AdCab dosage to 1×10^8 viral particles (vp), which is a 10-fold reduction from the 1×10^9 vp used previously.

Among the available murine models, we selected transgenic human CD89 mice with a BALB/c background, as these mice manifest a significantly higher number of neutrophils compared with other murine strains.[28] The use of this model showcased the feasibility of employing lower doses of adenovirus while maintaining therapeutic efficacy. This served as an initial step to establish a foundation for optimizing safe and effective adenovirus dosages in future human applications.[29] The results from the animal experiment suggested the potential of PeptiCab. This group exhibited the most effectively controlled tumor growth in comparison with control groups. The immunological data further revealed the presence of a greater number of memory antigen-specific CD8+T cells. Notably, a rapid transition from central memory to effector memory was observed in both the PeptiCRAd and PeptiCab groups. These findings confirmed that our therapeutic vaccination platform elicited antigen-specific antitumor T-cell responses, poised to transform into an effector phenotype on specific antigen stimulation.

The transgenic model provided us with an opportunity to gain a more comprehensive understanding of the role of neutrophils within our platform. Neutrophils are the most abundant circulating leukocytes in the bloodstream and serve as first responders at infection sites.[30] While their established role in combating infections is widely recognized, their potential as APCs remains an area of limited exploration. Nonetheless,

emerging evidence highlights that neutrophils can assume distinct phenotypes in response to environmental cytokines and chemokines. For instance, stimulation of neutrophils with GM-CSF (Granulocyte macrophage colony-stimulating factor) triggers the acquisition of APC-like attributes, such as upregulation of MHC-II, CD80, and CD86.[31] This transformative process culminates in the activation and expansion of CD8+T cells. Conversely, exposure to TGF-β (Transforming growth factor) in the immunosuppressive microenvironment of the tumor leads neutrophils to adopt an immunosuppressive phenotype, negatively impacting the expansion and tumor-killing capacity of CD8+T cells.[32] Neutrophils are characterized by two distinct subtypes, N-α and N-β, which each have unique functions. N-β neutrophils exhibit more pronounced lobulation and hypersegmentation than their N-α counterparts.[17 33] Moreover, N-β neutrophils exhibit increased APC-like functions, evidenced by elevated MHC-II and CD80/CD86 expression. In the context of vaccinia virus vaccination in mice, N-β neutrophils contribute significantly to the robust induction of CD8+T cell responses against the virus.[17 33] Remarkably, this effect hinges on the presence of myeloid DCs, indicating that N-β neutrophils are reliant on myeloid DCs to activate naïve CD8+T cells. This finding resonates with our own observations in CD89 TG, where administration of PeptiCab yields a more pronounced coordination of active and memory CD8+T cells compared with PeptiCRAd. The release of the cross-hybrid IgGA Fc-fusion peptide during PeptiCab administration potentially triggers the secretion of immunogenic cytokines and chemokines. Notably, in these mice, CD89 is expressed in the myeloid compartment (mimicking human expression patterns), and activation with IgA antibodies leads to potent ITAM activation when compared with IgG antibodies.[34] This robust activation likely synergizes with the functions of various APCs, including DCs, macrophages, and neutrophils, resulting in the upregulation of MHC-II and CD80/CD86. Consequently, this augmentation of the vaccine response culminates in heightened activation of both CD8+ and CD4+ T cells on exposure to the SYL peptide. These findings underscore the role of Fc receptors in orchestrating T-cell responses within a vaccination context. Furthermore, the use of IgA antibodies holds promise for enhancing such responses by bolstering neutrophils acquisition of the MHC-II phenotype.

AdCab may contribute to remodeling the TME. By targeting immunosuppressive PD-L1-expressing cells, the Fc-fusion peptide may enhance T-cell activation and expansion by reducing immune suppressive cells, such as myeloid suppressor cells, that may hinder antitumor responses. Furthermore, the interaction of the IgG portion of the Fc-fusion peptide with FcγRs on APCs may enhance antigen processing and cross-presentation. Activation of FcγRs triggers important changes in macrophages and DCs, including upregulation of both MHC-I and MHC-II and co-stimulatory molecules (CD80 and CD86), promoting efficient antigen presentation and T-cell activation.[12] Peptide-antibody complexes also induce the upregulation of pro-inflammatory cytokines (TNF-α, IFN-γ, IL-6, and IL-1β), which are critical for T-cell expansion, differentiation, and maturation.[35 36]

In our study, PeptiCab demonstrated a specific and robust antitumor response against the tumor peptide decorated on the oncolytic adenovirus. Notably, this response was more pronounced than that observed in mice treated with PeptiCRAd, underscoring the additive benefits of the Fc-fusion peptide in the vaccine. The enhanced antitumor response achieved with PeptiCab underscores the intricate interplay of passive antibody administration, FcγR engagement, and TME remodeling, which collectively leads to potent activation of antitumor T-cell responses. Our findings provide valuable insights into the mechanisms underpinning antitumor T-cell responses through FcγR engagement. Understanding the role of FcγRs in antigen presentation and cytokine release at the molecular level, combined with the impact on the TME, may pave the way to developing innovative cancer immunotherapies. The ability of PeptiCab to induce robust antitumor responses may hold promise to improve cancer vaccination strategies and in future clinical applications.

MATERIAL AND METHODS

Cell lines and reagents

The murine colon carcinoma cell line CT26 was cultured in RPMI-1640 (Roswell Park Memorial Institute); the murine melanoma cell line B16K1 was cultured in DMEM (Dulbecco's Modified Eagle Medium) high glucose; the murine triple-negative breast cancer cell line 4T1 was cultured in RPMI high glucose; and B16F10 cell line was cultured in DMEM. The human lung adenocarcinoma cell line A549 and human triple-negative breast cancer cell line MDAMB436 were cultured in DMEM. All the media were supplemented with 10% FBS (Gibco), 1% glutamine (Gibco), 100 µg/mL streptomycin, and 100 U/mL penicillin (Life Technology, California, USA). B16.OVA, a mouse melanoma cell line expressing chicken OVA, was kindly provided by Professor Richard Vile (Mayo Clinic, Rochester, Minnesota, USA). B16.OVA cells were cultured in RPMI with 10% FBS (Fetal bovine serum), 1% L-glutamine, 1% penicillin/streptomycin, and 5 mg/mL Geneticin (Life Technologies).

Cells were cultivated at 37°C, 5% CO_2 in a humidified atmosphere and routinely tested for *Mycoplasma* contamination.

The peptides used in the study were purchased from Chempeptides (Shanghai, China).

MTS assays

For cell viability, cells were plated at a density of 10,000 cells per well in a 96V bottom plate (Sarstedt) and then

infected at various MOIs (Multiplicity of infection) (0.01–100). Infected cells were then incubated for 3 days at 37°C. Cell death was assessed using an MTS kit according to the manufacturer's instructions (Cell Titer 96 AQueous One Solution Cell Proliferation Assay, Promega, Nacka, Sweden). Absorbance was then read using a Varioskan LUX Multimode Reader (Thermo Scientific)

Fc-fusion peptide production experiment

Murine and human cell lines were cultured in T175 culture flasks until confluent. Cells were infected with adenoviruses at 100 MOI. At the indicated time points, supernatants were collected and run through a His GraviTrap (Cytiva) due to the presence of an 8×His tag in the Fc-fusion peptides. Fractions containing Fc-fusion peptides were pooled and concentrated using Vivaspin concentration columns (100,000 MWCO; Sartorius). Fc-fusion peptide concentrations were calculated using the following formula:

$$\frac{OD\ value\ at\ 280nm}{1.4\left(Correction\ factor\right)}$$

ADCC assays

ADCC assays were performed by culturing targe T cells at a density of 15,000 cells per well in a 96-flat well plate (Sarstedt) and infected with adenovirus at an MOI of 100 for 48 hours. After the production of Fc-fusion peptides, effector cells were co-incubated at a ratio of 1:100 or 1:40 (target:effector) for PBMCs and PMNs, respectively. Serum was added at a final concentration of 15.5% to mimic physiological conditions. After 4 hours of incubation at 37°C, supernatant was collected and LDH (Lactate dehydrogenase) release was measured to calculate cell death. Specific percent cell lysis was calculated using the following formula:

$$\frac{\text{experimental LDH release}\ \ \text{effector plus target spontaneous}}{\text{target maximum}\ \ \text{effector plus target spontaneous}} X100$$

Experimental LDH release is the LDH released from treated samples. Effector plus target spontaneous LDH release is the LDH released from target cells co-incubated with effector cells without any treatment (virus). The target maximum corresponds to target cells treated with cell lysis buffer to determine the maximum LDH released.

Oncolytic adenovirus

The oncolytic adenovirus Ad5/3Δ24 and AdCab were used. Ad5/3Δ24 is a conditionally replicating adenovirus serotype 5 with adenovirus 3 fiber knob modification, carrying a 24-base pair deletion of the E1A gene. AdCab was generated according to Hamdan *et al*.[13] Briefly, the Fc-fusion peptide gene was inserted in the gp19k+7.1 region of the adenovirus using the Gibson Assembly method. The vp concentration was measured at 260 nm, and infection units were determined by immunocytochemistry by staining the hexon protein in infected A549 cells.

PeptiCab complex formation

The PeptiCab complex was prepared by mixing the adenoviral vector and peptide with a polyK tail. We mixed polyK-extended epitopes with the adenoviral vector for 15 min at room temperature before treatments with the PeptiCab complexes. Further details about the stability and formation of the complex have been described previously.[7] The amount for each peptide and for each virus used is shown in the figure legends for each experiment.

Murine IFN-γ ELISpot

IFN-γ ELISpot assays were performed using a commercially available mouse ELISpot reagent set (ImmunoSpot, Bonn Germany). A total of 0.01 mg/µL of each peptide and the equivalent amount of DMSO (Sigma) as a negative control were added for in vitro stimulations of 3×10^5 splenocytes for each well at 37°C for 72 hours. Spots were counted using an ELISpot reader system (ImmunoSpot, Bonn Germany). Data are expressed as IFN-γ spot-forming cells per 1×10^6 splenocytes. All the values were DMSO (Dimethyl sulfoxide) subtracted.

Intracellular stimulation and staining

A total of 2×10^6 murine splenocytes were incubated in a 96 U bottom well (Sarstedt) along with brefeldin A (1:1,000) and monensin A (1:1,000) at 37 °C for 5 hours. Stimulants were added at 2 µg and 40 MOI of peptides or adenovirus, respectively. After stimulation, samples were stored at 4°C overnight. Samples were then processed by centrifuging and resuspending pellets in murine Fc-block (BioLegend) at 4°C for 15 min. Extracellular proteins were then stained using the following panel: BV711 CD3 (BD Biosciences, #563123), BV510 CD8 (BD Biosciences, #563068), PE-CF594 CD4 (BD Biosciences, #562285), APC CD62L (eBioscience, #17-0621-81), AF700 CD44 (BioLegend, #103026) and v450 CCR7 (BD Biosciences, #560805). After staining, samples were fixed and permeabilized using a Fixation/Permeabilization kit (BD Biosciences) and following the manufacturer's instructions. Intracellular proteins were then stained with the following panel: BV650 TNF-α (BioLegend, #506333), PE-Cy7 IL-2 (BioLegend, #503832), PE IFN-γ (BioLegend, #505808) Perp-eFluor-710 (Invitrogen, #46-1541-82) and FITC IL-6 (BioLegend, #503806). Samples were then run on a Fortessa flow cytometer (BD Bioscience) and data was analyzed with FlowJo (FlowJo V.10.8.2)

Flow cytometry of tumor samples

Tumors from mice were passed through a 70 µm cell strainer (Falcon) to obtain a cell suspension. One million cells were then plated in a 96 V bottom well plate (Sarstedt) and stained with the following antibodies: BV711 CD11b (BioLegend, #101241), BV510 Ly6G (BioLegend, #108437), PE-FC594 (BioLegend, #124323), APC Siglec-F (BioLegend, #155507), AF700 MHC-II (BioLegend, #107621), FITC CD80 (BioLegend, #104705), BV650 CD86 (BioLegend, #105035), PE-Cy7 CD101 (Invitrogen, #25-1011-82) and PE CD89 (BioLegend, #354103).

Samples were run on a Fortessa flow cytometer (BD Bioscience). Data were analyzed with FlowJo (FlowJo V.10.8.2).

Animal experiments

For mice bearing B16K1 tumors, 0.1×10^6 cells were mixed with Matrigel (Matrigel matrix high protein, Corning) at ratio 1:1 and injected subcutaneously into the right flank. For mice bearing CT26 tumors, 1×10^6 and 0.6×10^6 cells were injected subcutaneously into the right and left flanks, respectively.

BM from wild-type C57/Bl and hCD89 TG were isolated by flushing femurs and tibiae with sterile PBS. BM was treated with ACK (Gibco) buffer and resuspended in PBS.

For the TG expressing human FcαRI (CD89), 0.6×10^6 cells were injected subcutaneously in the right flank. For the ACT experiment, splenocytes and BM were harvested from either TG C57BL/6 mice bearing human FcαRI (CD89) or from wild-type C57BL/6.

For CD8-depletion studies, mice were treated with 500 µg of anti-CD8 depletion antibody (Clone 2.43, Bio X Cell) I.P (Intraperitoneal injection) 1 day before the first treatment and then given 100 µg of anti-CD8 depletion antibody every other day for a total of two rounds.

A complete randomization was performed on the day of the treatment. Details on the schedule of the treatment can be found in the figure legends. The viral dose used was 1×10^9 vp/tumor complexed with 20 µg of a single peptide. The tumors were measured with a caliper and the mice were sacrificed when the human ethical endpoint was met.

Nano-tracking analyses

AdCab and PeptiCab were analyzed using NanoSight model LM14 (NanoSight) equipped with blue (404 nm, 70 mW) laser and SCMOS camera. Samples were diluted in PBS and three 60 s videos were recorded using camera level 13. Data were analyzed using NTA software V.3.0 with a detection threshold of 5 and screen gain of 10 to track as many particles as possible with minimal background.

Statistical analyses

Graphs were generated and statistical analyses were performed using GraphPad Prism V.9.0 software (GraphPad Software). Details on the statistical tests for each experiment can be found in the corresponding figure legends.

Neutrophil and CD8+T cell expansion

PBMCs and neutrophils were isolated from a buffy coat using a double-layer Histopaque-Ficoll gradient. Neutrophils were then left untreated or underwent an ADCC experiment with CT26 using the same methodology as explained above. CD8+T cells were then enriched using CD8 beads (130-045-201, Miltenyi) and labeled with CFSE (C34570, Invitrogen) according to the manufacturer's instructions. 500,000 neutrophils were then incubated with 500,000 CD8+T cells along with 2 µg of adenovirus peptides (130-098-237, Miltenyi) and 50 U/mL of IL-2 (78036, STEMCELL) in a 96 U bottom plate. After 4 days, CFSE was measured using a flow cytometry. FlowJo was used to analyze the data and calculate the expansion index.

Study approval

All animal experiments were reviewed and approved by the Experimental Animal Committee of the University of Helsinki and the Provincial Government of Southern Finland (license number ESAVI/12722/2022). Four-to-six weeks old female C57BL/6JOlaHsd and BALB/cOlaHsd mice were obtained from Envigo (Laboratory, Bar Harbor, Maine UK). C57BL/6JOlaHsd and BALB/cOlaHsd TG expressing human FcαRI (CD89) were kindly provided by the laboratory of Jeanette Leusen.

Data availability

All data generated in this manuscript are available on request.

Author affiliations
[1]University of Helsinki Faculty of Pharmacy, Laboratory of Immunovirotherapy, Drug Research Program Helsinki, Uusimaa, FI, Helsinki, Finland
[2]Helsinki Institute of Life Science (HiLIFE), Fabianinkatu 33, University of Helsinki, 00710 Helsinki, Finland, Helsinki, Finland
[3]Translational Immunology Program (TRIMM), Faculty of Medicine Helsinki University, Helsinki, Finland
[4]Digital Precision Cancer Medicine Flagship (iCAN), University of Helsinki, Helsinki, Finland
[5]Valo Therapeutics Oy, Helsinki, Finland
[6]Center for translational immunology, UMC Utrecht, Utrecht, The Netherlands
[7]Department of Molecular Medicine and Medical Biotechnology and CEINGE, Naples University Federico II, Naples, Italy

Twitter Vincenzo Cerullo @vincersurf

Contributors SF is listed as the first coauthor because she led the project as a senior scientist. SF, FH, and VC designed the study. SF, JC, FH, and MFu set-up, and optimized methodology. SF and FH performed experiments and related data analysis. GA, FD'A, and SR provided technical support. JL provided us with transgenic mice for hCD89. All the authors interpreted the results. SF and FH wrote the original manuscript draft and equally contributed as first authors. All authors read, corrected, and approved the final manuscript. VC supervised the study and acts as guarantor and accepts full responsibility for the work and/or conduct of the study, had access to the data, and controlled the decision to publish.

Funding This work was supported by the European Research Council under the European Union's Horizon 2020 Framework program (H2020)/ERC-CoG-2015 Grant Agreement No. 681219, the Helsinki Institute of Life Science (HiLIFE) (797011004), the Jane and Aatos Erkko Foundation (decision 19072019), the Cancer Society of Finland (Syöpäjärjestöt) (4706116) and the Sigrid Juséliuksen Säätiö (8090).

Competing interests VC is a co-founder and shareholder at VALO Therapeutics. SP is a co-founder, an employee, and a shareholder at VALO Therapeutics. VS is currently employed by AstraZeneca. The other authors have no conflicts of interest.

Patient consent for publication Not applicable.

Ethics approval Not applicable.

Provenance and peer review Not commissioned; externally peer reviewed.

Data availability statement Data are available upon reasonable request.

ORCID iDs
Sara Feola http://orcid.org/0000-0002-4012-4310
Firas Hamdan http://orcid.org/0000-0003-4678-7382
Salvatore Russo http://orcid.org/0000-0002-0287-0048
Manlio Fusciello http://orcid.org/0000-0002-7166-3018
Riikka Mölsä http://orcid.org/0009-0002-6800-4318
Jeanette Leusen http://orcid.org/0000-0003-4982-6914
Vincenzo Cerullo http://orcid.org/0000-0003-4901-3796

REFERENCES

1 Kazemi T, Younesi V, Jadidi-Niaragh F, *et al*. Immunotherapeutic approaches for cancer therapy: an updated review. *Artif Cells Nanomed Biotechnol* 2016;44:769–79.
2 Ura T, Okuda K, Shimada M. Developments in viral vector-based vaccines. *Vaccines (Basel)* 2014;2:624–41.
3 Capasso C, Hirvinen M, Garofalo M, *et al*. Oncolytic adenoviruses coated with MHC-I tumor epitopes increase the antitumor immunity and efficacy against melanoma. *Oncoimmunology* 2016;5:e1105429.
4 Feola S, Capasso C, Fusciello M, *et al*. Oncolytic vaccines increase the response to PD-L1 blockade in Immunogenic and poorly immunogenic tumors. *Oncoimmunology* 2018;7:e1457596.
5 Peltonen K, Feola S, Umer HM, *et al*. Therapeutic cancer vaccination with Immunopeptidomics-discovered antigens confers protective antitumor efficacy. *Cancers (Basel)* 2021;13:3408.
6 Feola S, Chiaro J, Martins B, *et al*. A novel immunopeptidomic-based pipeline for the generation of personalized oncolytic cancer vaccines. *Elife* 2022;11:e71156.
7 Ylösmäki E, Ylösmäki L, Fusciello M, *et al*. Characterization of a novel OX40 ligand and CD40 ligand-expressing oncolytic adenovirus used in the pepticrad cancer vaccine platform. *Mol Ther Oncolytics* 2021;20:459–69.
8 Regnault A, Lankar D, Lacabanne V, *et al*. Fcgamma receptor-mediated induction of dendritic cell maturation and major histocompatibility complex class I-restricted antigen presentation after immune complex internalization. *J Exp Med* 1999;189:371–80.
9 Dhodapkar KM, Krasovsky J, Williamson B, *et al*. Antitumor monoclonal antibodies enhance cross-presentation ofcCellular antigens and the generation of myeloma-specific killer T cells by dendritic cells. *J Exp Med* 2002;195:125–33.
10 Park S, Jiang Z, Mortenson ED, *et al*. The therapeutic effect of anti-HER2/neu antibody depends on both innate and adaptive immunity. *Cancer Cell* 2010;18:160–70.
11 de Bono JS, Rha SY, Stephenson J, *et al*. Phase I trial of a murine antibody to MUC1 in patients with metastatic cancer: evidence for the activation of humoral and cellular antitumor immunity. *Ann Oncol* 2004;15:1825–33.
12 Junker F, Gordon J, Qureshi O. Fc gamma receptors and their role in antigen uptake, presentation, and T cell activation. *Front Immunol* 2020;11:1393.
13 Hamdan F, Ylösmäki E, Chiaro J, *et al*. Novel oncolytic adenovirus expressing enhanced cross-hybrid Igga FC PD-L1 inhibitor activates multiple immune effector populations leading to enhanced tumor killing in vitro, in vivo and with patient-derived tumor organoids. *J Immunother Cancer* 2021;9:e003000.
14 Hamdan F, Feodoroff M, Russo S, *et al*. Controlled release of enhanced cross-hybrid Igga FC PD-L1 inhibitors using oncolytic adenoviruses. *Mol Ther Oncolytics* 2023;28:264–76.
15 Bournazos S, Wang TT, Ravetch JV. The role and function of Fcgamma receptors on myeloid cells. *Microbiol Spectr* 2016;4.
16 Treffers LW, van Houdt M, Bruggeman CW, *et al*. Fcgammariiib restricts antibody-dependent destruction of cancer cells by human neutrophils. *Front Immunol* 2018;9:3124.
17 Beauvillain C, Delneste Y, Scotet M, *et al*. Neutrophils efficiently cross-prime naive T cells in vivo. *Blood* 2007;110:2965–73.
18 Ashtekar AR, Saha B. Poly's plea: membership to the club of APCs. *Trends Immunol* 2003;24:485–90.
19 Vono M, Lin A, Norrby-Teglund A, *et al*. Neutrophils acquire the capacity for antigen presentation to memory CD4(+) T cells in vitro and ex vivo. *Blood* 2017;129:1991–2001.
20 Kovacsovics-Bankowski M, Clark K, Benacerraf B, *et al*. Efficient major histocompatibility complex class I presentation of exogenous antigen upon phagocytosis by macrophages. *Proc Natl Acad Sci U S A* 1993;90:4942–6.
21 Aderem A, Underhill DM. Mechanisms of phagocytosis in macrophages. *Annu Rev Immunol* 1999;17:593–623.
22 Dhodapkar KM, Kaufman JL, Ehlers M, *et al*. Selective blockade of inhibitory Fcgamma receptor enables human dendritic cell maturation with IL-12P70 production and immunity to antibody-coated tumor cells. *Proc Natl Acad Sci U S A* 2005;102:2910–5.
23 DiLillo DJ, Ravetch JV. Differential FC-receptor engagement drives an anti-tumor vaccinal effect. *Cell* 2015;161:1035–45.
24 Han J, Khatwani N, Searles TG, *et al*. Memory CD8(+) T cell responses to cancer. *Semin Immunol* 2020;49:101435.
25 Pittet MJ, Speiser DE, Liénard D, *et al*. Expansion and functional maturation of human tumor antigen-specific CD8+ T cells after vaccination with antigenic peptide. *Clin Cancer Res* 2001;7:796s–803s.
26 Tietze JK, Angelova D, Heppt MV, *et al*. The proportion of circulating CD45Ro(+)CD8(+) memory T cells is correlated with clinical response in melanoma patients treated with Ipilimumab. *European Journal of Cancer* 2017;75:268–79.
27 Pedicord VA, Montalvo W, Leiner IM, *et al*. Single dose of anti-CTLA-4 enhances CD8+ T-cell memory formation, function, and maintenance. *Proc Natl Acad Sci U S A* 2011;108:266–71.
28 Stip MC, Jansen JHM, Nederend M, *et al*. Characterization of human FC alpha receptor transgenic mice: comparison of CD89 expression and antibody-dependent tumor killing between mouse strains. *Cancer Immunol Immunother* 2023;72:3063–77.
29 Afrough S, Rhodes S, Evans T, *et al*. Immunologic dose-response to adenovirus-vectored vaccines in animals and humans: a systematic review of dose-response studies of replication incompetent adenoviral vaccine vectors when given via an intramuscular or subcutaneous route. *Vaccines (Basel)* 2020;8:131.
30 Mantovani A, Cassatella MA, Costantini C, *et al*. Neutrophils in the activation and regulation of innate and adaptive immunity. *Nat Rev Immunol* 2011;11:519–31.
31 Matsushima H, Geng S, Lu R, *et al*. Neutrophil differentiation into a unique hybrid population exhibiting dual phenotype and functionality of neutrophils and dendritic cells. *Blood* 2013;121:1677–89.
32 Fridlender ZG, Sun J, Kim S, *et al*. Polarization of tumor-associated neutrophil phenotype by TGF-beta: "N1" versus "N2" TAN. *Cancer Cell* 2009;16:183–94.
33 Di Pilato M, Mejías-Pérez E, Zonca M, *et al*. Nfkappab activation by modified Vaccinia virus as a novel strategy to enhance neutrophil migration and HIV-specific T-cell responses. *Proc Natl Acad Sci U S A* 2015;112:E1333–42.
34 Brandsma AM, Bondza S, Evers M, *et al*. Potent FC receptor signaling by IgA leads to superior killing of cancer cells by neutrophils compared to IgG. *Front Immunol* 2019;10:704.
35 Junker F, Krishnarajah S, Qureshi O, *et al*. A simple method for measuring immune complex-mediated, FC gamma receptor dependent antigen-specific activation of primary human T cells. *J Immunol Methods* 2018;454:32–9.
36 Qureshi OS, Rowley TF, Junker F, *et al*. Multivalent Fcgamma-receptor engagement by a hexameric FC-fusion protein triggers Fcgamma-receptor internalisation and modulation of Fcgamma-receptor functions. *Sci Rep* 2017;7:17049.